Analysis of neutrino fluxes from cosmic rays interactions in the Earth's atmosphere

Mihail Chizhov[1,2], Peter Danev[1]
[1] Faculty of Physics, Sofia University, 1164 Sofia,Bulgaria
[2] Joint Institute for Nuclear Research, 141980 Dubna, Russia
mih@phys.uni-sofia.bg
(Submitted on 30.05.2013; Accepted on 16.06.2013)

Abstract. The cosmic rays have a glorious century long history. They are an inexhaustible source of fundamental knowledge and practical applications. In this paper we have studied properties of neutrino fluxes which have originated from cosmic rays interactions in the Earth's atmosphere. Upward going neutrinos propagating through the Earth can undergo oscillation phenomena in matter. Therefore, knowledge of neutrino fluxes can help for the determination of the unknown yet neutrino parameters. Several useful analytical formulae have been obtained.
Key words: cosmic rays, atmospheric neutrino fluxes, Earth's matter effect

Introduction

The discovery of cosmic rays (CRs) by Victor Hess in August 1912 opened a new window into high energy and particle physics. Many discoveries of new particles in the CRs have been made, which allow us to extent our knowledge about fundamental structure of Nature. For some period of time the CRs were the only source of high energy accelerated particles. Even after launching of new high-power terrestrial accelerators careful analysis of CRs interactions in emulsion (Niu 2008) allows us to observe new particles: a bound state from *charm* quarks, before such state has been discovered on hadron (Aubert 1974) and lepton (Augustin 1974) accelerators. Besides fundamental discoveries, cosmic rays also find practical applications. For example, the cosmic muons have been always used for detector calibration.

Even today CRs provide us with unprecedentedly high-energy accelerated particles, unreachable at present terrestrial laboratories, and serve as additional natural source of various particle beams propagating in different directions. That is why the study of CRs properties is very important. Thus, large detectors such as IMB (Casper 1991; Becker-Szendy 1992), Kamiokande (Hirata 1988, 1992; Fukuda 1994), Soudan-2 (Allison 1997) and MACRO (Ambrosio 1998) observed a deficit in the ratio of the fluxes of muon to electron atmospheric neutrinos in comparison with theoretical predictions. Further very precise measurements by Super-Kamiokande Collaboration (Fukuda 1998) gave the first experimental evidence for atmospheric neutrino oscillations in 1998.

Neutrino oscillations were proposed by Bruno Pontecorvo (Pontecorvo 1957, 1958) in analogy with the $K^0 - \bar{K}^0$ oscillations (see also Maki 1962). The pattern of oscillations of ultra-relativistic neutrinos in vacuum depends in the simplest case of two neutrino types on two neutrino parameters: the vacuum mixing angle ϑ and the neutrino squared mass difference Δm^2, and also on the neutrino energy E and the distance L traveled by the neutrinos. So, the probability of transition between two different weak-eigenstate neutrinos

$$P_2 = \sin^2 2\vartheta \, \sin^2 \frac{\varphi}{2} \tag{1}$$

is determined by the mixing angle 2ϑ and the phase $\varphi = 2\pi L/L_0$, where $L_0 = 2.48(E/\mathrm{GeV})/(\Delta m^2/\mathrm{eV}^2)$ km is the oscillation length in vacuum.

Due to Earth's geometry the baseline of neutrino propagation from creation point to detection point varies from 20 km up to 12,800 km for different directions. It enables experiments to be sensitive to very broad region of neutrino oscillation parameters.[1] The experimental data point to disappearance of the muon neutrinos, ν_μ, with approximately maximum mixing angle (Abe, 2011). The global analysis (Fogli 2012) gives $\sin^2 2\vartheta_{\mathrm{atm}} \approx 0.95$ and $|\Delta m^2_{\mathrm{atm}}| \approx 2.4 \times 10^{-3}$ eV^2. It is important to note that neither the octant of the mixing angle, ϑ_{atm}, nor $\Delta m^2_{\mathrm{atm}}$ sign cannot be determined from eq. (1). It has been found also that muon neutrinos oscillate into tau neutrinos (Fukuda 2000; Abe 2006).[2] For such type of oscillations eq. (1) is still valid in matter.

However, when neutrinos propagate in matter, which consists of particles only from the first generation, an additional phase difference can arise between the electron and other neutrino flavours, such as muon or tau neutrinos, due to additional exchange through W boson. Namely with this MSW effect (Mikheyev&Smirnov 1985; Wolfenstein 1978) the solar neutrino anomaly (Davis 1972) can be explained. At present the neutrino parameters connected with the solar problem are $\sin^2\vartheta_{\mathrm{sol}} \approx 0.307$ and $\Delta m^2_{\mathrm{sol}} \approx 7.54 \times 10^{-5}$ eV^2 (Fogli 2012). In general, three-neutrino mixing are parameterized in addition by the third mixing angle $\sin^2 2\vartheta_{\mathrm{react}} \approx 0.092$, measured recently very precisely in reactor experiment (An 2012), and unknown yet CP violation phase δ.

It has been shown (Chizhov 2001) that in the real case of $\Delta m^2_{\mathrm{sol}} \ll |\Delta m^2_{\mathrm{atm}}|$ the three-neutrino mixing is reduced to two flavour case:

$$P(\nu_e \to \nu_e) = 1 - P_2^m, \tag{2}$$

$$P(\nu_e \to \nu_\mu) = P(\nu_\mu \to \nu_e) = \sin^2\vartheta_{\mathrm{atm}}\, P_2^m, \tag{3}$$

$$P(\nu_e \to \nu_\tau) = P(\nu_\tau \to \nu_e) = \cos^2\vartheta_{\mathrm{atm}}\, P_2^m, \tag{4}$$

$$P(\nu_\mu \to \nu_\mu) = 1 - \frac{1}{2}\sin^2 2\vartheta_{\mathrm{atm}}\left(1 - \sqrt{1 - P_2^m}\cos\phi\right) - \sin^4\vartheta_{\mathrm{atm}}\, P_2^m, \tag{5}$$

$$P(\nu_\mu \to \nu_\tau) = P(\nu_\tau \to \nu_\mu) = \frac{1}{2}\sin^2 2\vartheta_{\mathrm{atm}}\left(1 - \sqrt{1 - P_2^m}\cos\phi - \frac{1}{2}P_2^m\right), \tag{6}$$

$$P(\nu_\tau \to \nu_\tau) = 1 - \frac{1}{2}\sin^2 2\vartheta_{\mathrm{atm}}\left(1 - \sqrt{1 - P_2^m}\cos\phi\right) - \cos^4\vartheta_{\mathrm{atm}}\, P_2^m, \tag{7}$$

where

$$P_2^m = \sin^2 2\vartheta^m\, \sin^2\frac{\varphi^m}{2} \tag{8}$$

is the modified transition probability (1) in matter, ϕ is the known phase factor.

[1] So, for maximal baseline and 10 GeV neutrinos squared mass differences up to 10^{-3} eV^2 can be probed.

[2] This result is in agreement with constraints following from cosmological considerations (Barbieri&Dolgov 1991).

In the case of matter with constant density and chemical composition

$$\sin^2 2\vartheta^m = \frac{\sin^2 2\vartheta_{\rm react}}{\left(\cos 2\vartheta_{\rm react} - \dfrac{E\Delta V}{\Delta m^2_{\rm atm}}\right)^2 + \sin^2 2\vartheta_{\rm react}}, \tag{9}$$

and $\varphi^m = 2\pi L/L_m$, where the oscillation length in matter $L_m = 2.48(E/\mathrm{GeV})/(\Delta m^2_{\rm eff}/\mathrm{eV}^2)$ km is expressed through the effective squared mass difference

$$\Delta m^2_{\rm eff} = \Delta m^2_{\rm atm}\sqrt{\left(\cos 2\vartheta_{\rm react} - \frac{E\Delta V}{\Delta m^2_{\rm atm}}\right)^2 + \sin^2 2\vartheta_{\rm react}}. \tag{10}$$

Here the effective potential difference $\Delta V = \pm 2\sqrt{2} G_F N_A Y_e \rho$ is defined by the matter density ρ and its electron fraction number Y_e, and also by the universal Fermi coupling constant, G_F, and Avogadro constant, N_A. The upper sign in ΔV corresponds to neutrino propagation and the bottom one – to antineutrino. Sign correlation between ΔV and $\Delta m^2_{\rm atm}$ can lead to resonant enhancement of the first multiplier in (8) for neutrino in the case of the normal hierarchy (NH) $\Delta m^2_{\rm atm} > 0$ or for antineutrino in the case of the inverse hierarchy (IH) $\Delta m^2_{\rm atm} < 0$.

The two-layer model of the Earth's interior is very appropriate for such type of approximation, where the mantle (3480 km $< R <$ 6371 km) and the core ($R <$ 3480 km) can be treated with approximately constant densities, $\rho_m \approx 5.0$ g/cm^3 and $\rho_c \approx 11.5$ g/cm^3, and the electron fraction number, $Y_e \approx 0.5$. In this case the resonant neutrino/antineutrino energy in the mantle is approximately 6 GeV ($\vartheta_m = \pi/4$) and the oscillation length $L_m \approx 20,800$ km. Therefore, for the given resonant energy and baseline $L_m/2 \approx 10,400$ km ($\varphi_m = \pi$), which corresponds to the neutrino upward direction with nadir angle approximately 35.2°, the electron neutrinos undergo total disappearance $P(\nu_e \to \nu_e) = 0$. The resonance width is very broad in nadir angle: from 0° up to 66.4°, and very restricted in energy: from 5 GeV up to 8 GeV.

For the neutrino trajectories crossing the mantle and the Earth's core with nadir angle less than 33.1° a new matter effect is operative. It has been shown (Chizhov&Petcov 1999) that especially due to that effect the total neutrino conversion is possible when neutrino propagates through multi-layer medium of nonperiodic constant density layers even when the MSW resonance conditions do not hold in any layer. In the case of mantle-core-mantle crossing the new resonance conditions are possible:

$$\begin{aligned}
\tan\frac{\varphi^m_{\rm mantle}}{2} &= \pm\sqrt{\frac{-\cos 2\vartheta^m_{\rm core}}{\cos(2\vartheta^m_{\rm core} - 4\vartheta^m_{\rm mantle})}},\\
\tan\frac{\varphi^m_{\rm core}}{2} &= \pm\frac{\cos 2\vartheta^m_{\rm mantle}}{\sqrt{-\cos 2\vartheta^m_{\rm core}\cos(2\vartheta^m_{\rm core} - 4\vartheta^m_{\rm mantle})}},
\end{aligned} \tag{11}$$

which are realized only for

$$\cos 2\vartheta^m_{\rm core} < 0 \tag{12}$$

$$\cos(2\vartheta^m_{\rm core} - 4\vartheta^m_{\rm mantle}) > 0. \tag{13}$$

It means that the new effect of the total neutrino conversion can take place only for neutrino energies between the resonant neutrino energy in core 2.6 GeV (condition (12)) and 7.6 GeV, which follows from cubic equation of the condition (13). Therefore, in the following we will concentrate mainly on this energy region and upward going neutrinos.

From previous considerations it can be seen that the matter effect $P_2^m \sim 1$ is operative in restricted regions of energy and nadir angle and has not been yet detected. Nevertheless, this effect can address hierarchy problem and can resolve octant degeneracy. Let us assume, that we know original atmospheric neutrino fluxes for all neutrino types: $\Phi^0_{\nu_e}$, $\Phi^0_{\nu_\mu}$ and $\Phi^0_{\nu_\tau}$. The initial tau neutrino flux $\Phi^0_{\nu_\tau}$ is negligible and we could safely neglect it in the following. Then the real neutrino fluxes after neutrino oscillation in the Earth can be given by the following expressions:

$$\begin{aligned}\Phi_{\nu_e} &= \Phi^0_{\nu_e} P(\nu_e \to \nu_e) + \Phi^0_{\nu_\mu} P(\nu_\mu \to \nu_e) \\ &= \Phi^0_{\nu_\mu} r \left[1 + \left(\frac{\sin^2\vartheta_{\rm atm}}{r} - 1\right) P_2^m\right], \end{aligned} \tag{14}$$

$$\begin{aligned}\Phi_{\nu_\mu} &= \Phi^0_{\nu_e} P(\nu_e \to \nu_\mu) + \Phi^0_{\nu_\mu} P(\nu_\mu \to \nu_\mu) \\ &= \Phi^0_{\nu_\mu} \left[1 - \frac{1}{2}\sin^2 2\vartheta_{\rm atm}\left(1 - \sqrt{1 - P_2^m}\cos\phi\right)\right. \\ &\quad \left. - r\sin^2\vartheta_{\rm atm}\left(\frac{\sin^2\vartheta_{\rm atm}}{r} - 1\right) P_2^m\right], \end{aligned} \tag{15}$$

$$\begin{aligned}\Phi_{\nu_\tau} &= \Phi^0_{\nu_e} P(\nu_e \to \nu_\tau) + \Phi^0_{\nu_\mu} P(\nu_\mu \to \nu_\tau) \\ &= \frac{1}{2}\,\Phi^0_{\nu_\mu}\sin^2 2\vartheta_{\rm atm}\left[1 - \sqrt{1 - P_2^m}\cos\phi\right. \\ &\quad \left. - \frac{r}{2\sin^2\vartheta_{\rm atm}}\left(\frac{\sin^2\vartheta_{\rm atm}}{r} - 1\right) P_2^m\right], \end{aligned} \tag{16}$$

where $r = \Phi^0_{\nu_e}/\Phi^0_{\nu_\mu}$.

Roughly $\sin^2\vartheta_{\rm atm} \sim r \sim 1/2$ and the matter effect is suppressed by the factor $\sin^2\vartheta_{\rm atm}/r - 1$ (see (14), (15) and (16)). Therefore, any deviation of the atmospheric mixing angle from the maximal value and the fluxes ratio from its naive estimation can be measured trough the matter effect. In the following we will be mainly interested in the flux ratio and we will give its useful parametrization.

1. Atmospheric neutrinos

Atmospheric neutrinos are produced by the interaction of the primary cosmic radiation with the Earth's atmosphere. The process of calculation of the

neutrino fluxes follows few basic steps. First un absolute primary cosmic ray flux has to be used. There are several effects that have to be calculated before this flux is fed to the hadronic simulation code. One of them is the solar activity and the other – reflection of cosmic rays in the Earth's magnetic field or rigidity cutoff. Widely accepted way to do that is the back-tracking technique explained in the following subsections. Then the nuclear reactions are simulated by a Monte Carlo program. If a 3D model is used, the effect of bending of charged particles in the geomagnetic field is applied for the secondary particles. The last step is counting the neutrinos passing through properly simulated detector.

1.1 Cosmic rays

The cosmic rays are high energy particles with energy up to 10^{20} eV. The maximum energy of the CRs nuclei depends on the charge of the corresponding nucleus. Thus, the high energy CRs have greater component of heavier nuclei and at energy $E \sim 10^{17}$ eV the spectrum is dominated by iron nuclei. At present it is believed that, at least up to the "knee" energy – 3×10^{15} eV, the CRs are produced in a diffusive acceleration applied to the strong outer shocks in the supernova remnants (SNRs). The CRs spectrum $N_n(E)$ is formed during the active period of SNRs until the supernova shock becomes too weak and therefore unable to accelerate more particles. The CRs with $E > 10^{18}$ eV have predominantly extragalactic origin. CRs from SNRs and the extragalatic component are enough to explain the entire galactic CR spectrum. The spectrum of CRs could be described by a power law. The emitted flux for the n-type nucleus has the following power law spectrum

$$N_n(E) \propto E^{-\gamma}. \tag{17}$$

The value of the slope $\gamma = 2 \div 2.4$ is estimated from the theory of SNRs. To get the correct value for the CRs flux measured at Earth, we have to include a diffusion coefficient $D(E)$

$$D(E) \propto E^{\delta},\ \delta \sim 0.6. \tag{18}$$

Finally, we get the CR flux

$$n(E) \propto \frac{N_n(E)}{D(E)} \propto E^{-\gamma-\delta} \simeq E^{-2.7}, \tag{19}$$

a power law that coincides with the one obtained by the experiments. For energies above the "knee" the spectrum changes to $n(E) \propto E^{-3}$. For detailed information on CRs see Berezhko&Völk (2007), Blasi&Amato (2012), Gaisser (2005) and Kang (2011).

The CRs in the low energy region, up to 100 GeV/nucleon, are known with relatively good precision thanks to the numerous Balloon-borne, satellite and ground-based experiments - AMS (Alpha Magnetic Spectrometer) (Alcaraz 2000), BESS (Balloon-borne Experiment with Superconducting Spectrometer) (Sanuki 2000), CAPRICE (Boezio 2003), PAMELA (Adriani 2009) and

many others. These particles responsible for neutrinos with energy less than 10 GeV have the following nuclei composition: $H^+ \sim 95.2\%$, $^2He^{++} \sim 4.5\%$, CNO nuclei $\sim 0.3\%$ and a negligible percentage of heavier nuclei (Honda 1995).

In the following we will use mainly more precise Honda (2011) results for India-based Neutrino Observatory (INO) site. A comparison with other groups and sites will be also presented. Honda (2011) are using a primary flux model based on AMS and BESS data.

1.2 Solar activity effect

The primary cosmic ray flux is also modified by the solar wind which varies with the 11-year solar cycle. The sun emits a magnetized plasma with a velocity of 100 - 200 km/s (Page&Marsden 1997). In the periods of a solar maximum, the plasma wind from the Sun highly suppresses incoming low-energy CRs and as a result primary cosmic flux is lowered. The solar wind stops the low energy cosmic rays to enter the upper layers of the atmosphere and interact with the air. And the higher energy particles ($\lesssim$ 30 GeV) lose energy in a process known as solar modulation. The effect is commonly parameterized by the sun-spot number or the count rate of neutron monitors.

This effect is the most noticeable for particles with energy less than 10 GeV. The net result is that neutrinos with energy 1 GeV and below have up to a few percent flux variation due to the solar cycle (see Fig. 1).

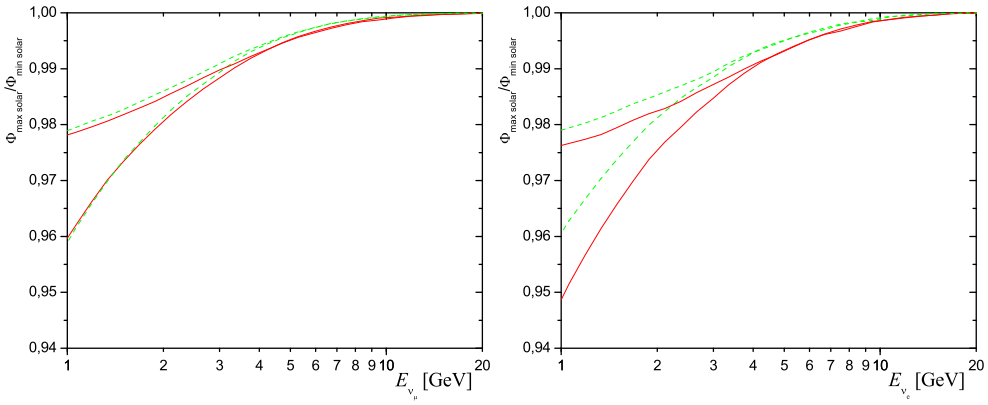

Fig. 1. The ratios of the muon (left) and electron (right) neutrino (solid) and antineutrino (dashed) fluxes at INO site in solar maximum and solar minimum for upward going neutrinos (upper curves) and the most affected fluxes at nadir angles around of 50° (bottom curves) are shown.

For neutrinos with energy of 10 GeV and more, this effect is negligible. In the following we will use averaged fluxes over solar cycle, since the solar activity effect is well within the calculation precision of 1% for interesting neutrino energy region around 6 GeV.

1.3 Rigidity cutoff

Outside the Earth's magnetic field CRs are almost isotropical. However the primary CRs are strongly affected by the Earth's magnetic field depending on location and propagation direction. While near the geomagnetic poles particles with very low momenta can penetrate to the Earth's surface, protons with up to 60 GeV, impinging horizontally near the geomagnetic equator are reflected back to space.

Earth's magnetic field could be approximated by a dipole and it has a slow variation with time. Thus, it is advisable to use the up-to-date model of the field (Finlay 2010). Its magnitude at the Earth's surface ranges from 25 to 65 μT. In the paper of Honda (2011) the geomagnetic field has been represented by multipole expansion of the spherical harmonic function. The International Geomagnetic Reference Field (IGRF2005) model (ver. 10) has been used with the only extrapolation available in 2010 (at the time of computation). The differences in the neutrino fluxes for different sites can been seen in Fig. 2.

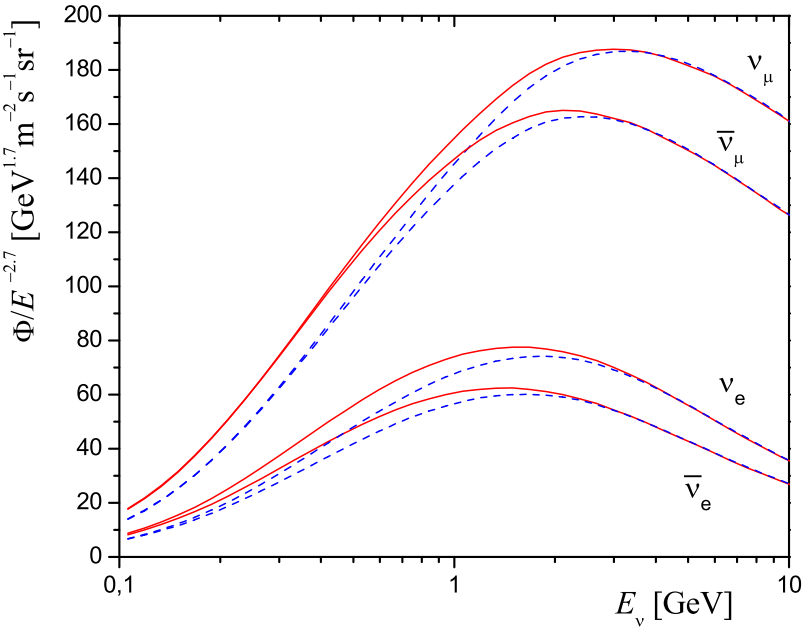

Fig. 2. The average neutrino fluxes with nadir angle between 0° and 60° at INO (solid curves) and Soudan (dashed curves) sites.

There are two effects caused by the geomagnetic field. First, it reflects primary cosmic rays of low rigidity ($R = p/q$, where p is the particle's momentum and q - its charge) and in that way prevents them from interacting with the air nuclei. The second effect is the bending of the charged particles in the atmosphere. Rigidity cutoff is most strong for the cosmic rays up to tens of GeV. Thus, the neutrino flux that is a product of these particles have an altitude and azimuth anisotropy. The energy of these neutrino is few GeV or less. Recently, Athar (2013) have calculated the neutrino fluxes for several sites by taking in account the horizontal component of the Earth's magnetic field. It can be seen that the east-west anisotropy could be quite large at INO site, where the strength of the horizontal component of geomagnetic field is the largest on the Earth.

The process of calculating rigidity cutoff is the following. For one-dimensional (1D) scheme, it is simple rejection of the primary cosmic rays with low rigidity. It is more complicated for three-dimensional (3D) calculations. First, the Earth is taken as a sphere with radius $R = 6378.180$ km. This approximation adds only a small uncertainty - less than 1%. Normally three more virtual spheres are introduced: the injection sphere, the simulation sphere, and the escape sphere with radius $R < R_{inj} < R_{sim} \leq R_{esc}$. Then the cosmic rays are sampled at injection sphere and a back-tracking is performed. Equation of motion is solved for these particles in time reversed direction. If they pass the escape sphere without touching the injection sphere again, that means that they can enter in the atmosphere and will not be reflected by the Earth's magnetic field. The cosmic rays path is simulated between simulation sphere and Earth's surface. The particles that enter the crust loose energy very quickly and cannot produce high energy neutrinos.

1.4 Hadronic interactions in the atmosphere

When the cosmic rays (primary p, n and ${}^2\mathrm{He}^{++}$) interact with the atoms of the Earth's atmosphere high energy mesons are produced. For example

$$p + N \rightarrow \pi^{\pm} + X. \tag{20}$$

Here N is an air nucleus – typically nitrogen and oxygen. Then these mesons decay to leptons. In order a neutrino with energy of few GeV to be produced, the most frequent processes are

$$\pi^{\pm} \rightarrow \mu^{\pm} + \nu_{\mu}(\bar{\nu}_{\mu}) \tag{21}$$

$$\mu^{\pm} \rightarrow e^{\pm} + \nu_e(\bar{\nu}_e) + \bar{\nu}_{\mu}(\nu_{\mu}). \tag{22}$$

Kaons are also created in the atmosphere by cosmic rays. They participate to neutrino production from the following reactions:

$$\begin{aligned} K^{\pm} &\to \mu^{\pm} + \nu_{\mu}(\bar{\nu}_{\mu}) \\ K^{\pm} &\to \pi^0 + \mu^{\pm} + \nu_{\mu}(\bar{\nu}_{\mu}) \\ K^{\pm} &\to \pi^0 + e^{\pm} + \nu_e(\bar{\nu}_e) \\ K_L^0 &\to \pi^+ + \pi^0 + \pi^- \\ K_L^0 &\to \pi^{\mp} + \mu^{\pm} + \nu_{\mu}(\bar{\nu}_{\mu}) \\ K_L^0 &\to \pi^{\mp} + e^{\pm} + \nu_e(\bar{\nu}_e). \end{aligned} \tag{23}$$

About 10% of the atmospheric neutrinos are created in these processes as well as in the subsequent decays of pions and muons. Other high energy particles also could create neutrinos but with energy higher than hundreds of TeV.

There are different Monte Carlo models for calculating the hadronic interactions used by various groups Honda (2011), Battistoni (2003), Barr (2004) – NUCRIN (Hänssgen&Ranft 1986), JAM (used in Particle and Heavy-Ion Transport code System (PHITS) (Niita, 2006)), DPMJET (Roesler 2000), COSMOS (Kasahara&Torii 1991), FRITIOF (Nilsson-Almqvist&Stenlund 1987) and others. In the paper of Athar (2013) for simulation of hadronic processes ATMNC (ATmospheric Muon Neutrino Calculation) code with JAM is used. JAM code has shown a little better agreement for the value of muon fluxes with the HARP experiment (Catanesi 2008) than with the alternative hadronic interaction model DPMJET-III (Roesler 2000) in the energy region below 32 GeV. For higher energies DPMJET-III model is used.

In these calculations the atmosphere density profile has major impact on the neutrino fluxes due to several reasons. Knowledge about of constituents of the air and their ratios for all altitudes in the simulation sphere is important in order to simulate a good cascade. The atmosphere density profile is also the reason for a large zenith angle dependence of the neutrino fluxes (Honda 1995). Another effect is that the secondary particles are loosing energy by propagating in the air. The uncertainty in the neutrino flux could be as high as 5%, but yearly averaged fluxes have less dependence on the atmosphere profile. For example, in the article Athar (2013) NRLMSISE-00 atmosphere model (Picone 2002) is used.

1.5 Counting the neutrinos. Virtual detector.

There is a difference in the way the neutrinos for each site are counted that depends on the used calculation scheme. In the one-dimensional scheme, all interactions and decay products follow the direction of the incident cosmic-ray particle that produced them. It is a simple model because it uses the assumption that the produced neutrino follows the path of the primary cosmic ray. This approximation is more reliable for high energy CRs and calculations are far less time consuming, than in full three-dimensional scheme.

When the 3D calculations are used, the effects of the secondaries bending in the geomagnetic field and their transverse momentum have to be calculated. Muons have a long path in the atmosphere, thus the impact of the geomagnetic

field to their movement have important consequences for the neutrino fluxes. The difference between 1D and 3D schemes is that within the second scheme there is an enhancement of the neutrino flux near the horizon. This feature is absent in 1D calculation.

Neutrino detectors are very small compared with the size of the Earth. However, in order to have enough statistic in the 3D scheme, a finite size "virtual detector" for each target detector is introduced (Honda 2007). It typically has circular or rectangular shape and dimensions of hundreds or thousands kilometers. The use of a virtual detector introduces an error. To minimize it, we should make a correction. If we have a circular virtual detector with radius θ_d, the neutrino flux through it could be written as

$$\Phi_{\theta_d} = \Phi_0 + \Phi'_0 \theta_d^2.$$

Assuming two virtual detectors with radii θ_1 and θ_2, the flux at the target detector Φ_0 can be calculated as

$$\Phi_0 = \frac{\Phi_2 \theta_1^2 - \Phi_1 \theta_2^2}{\theta_1^2 - \theta_2^2}.$$

A detailed explanation of the "virtual detector correction" could be found in Honda (2007). The statistical uncertainty due to this correction is typically less than 1%.

2. Flux analysis and results

We will analyse the atmospheric neutrino fluxes calculated by several groups: Honda (2011), Barr (2004), Battistoni (2003). As it was explained in the Introduction we are mainly interested in the ratio of electron to muon neutrinos. Therefore, we will investigate how this ratio depends on the azimuthal and nadir angles, different detector location on the Earth and calculations of the different groups. All these studies we will perform for restricted neutrino parameter region of our interest. In order to have maximal matter effect in the Earth we will analyse only upward going neutrinos with energy from 1 to 10 GeV.

2.1 East-West asymmetry

In a recent paper of Athar (2013) the authors have shown that for some parts of the Earth's surface the azimuthal angle dependence of atmospheric neutrino flux is substantial for the neutrino with an energy of a few GeV. One such place, where the strength of the horizontal component of geomagnetic field is close to the largest onthe Earth, is INO site. We will analyze an opportunity of using the azimuthal anisotropy to enhance sensitivity to the matter effect.

In Fig. 3 and Fig. 4 we have shown the effect of the azimuthal asymmetry for INO site. As mentioned before this is the place where this effect is maximal. We have drawn 12 curves for different azimuthal directions with different color corresponding to each 30° bin. The reddish (dashed) curves correspond to

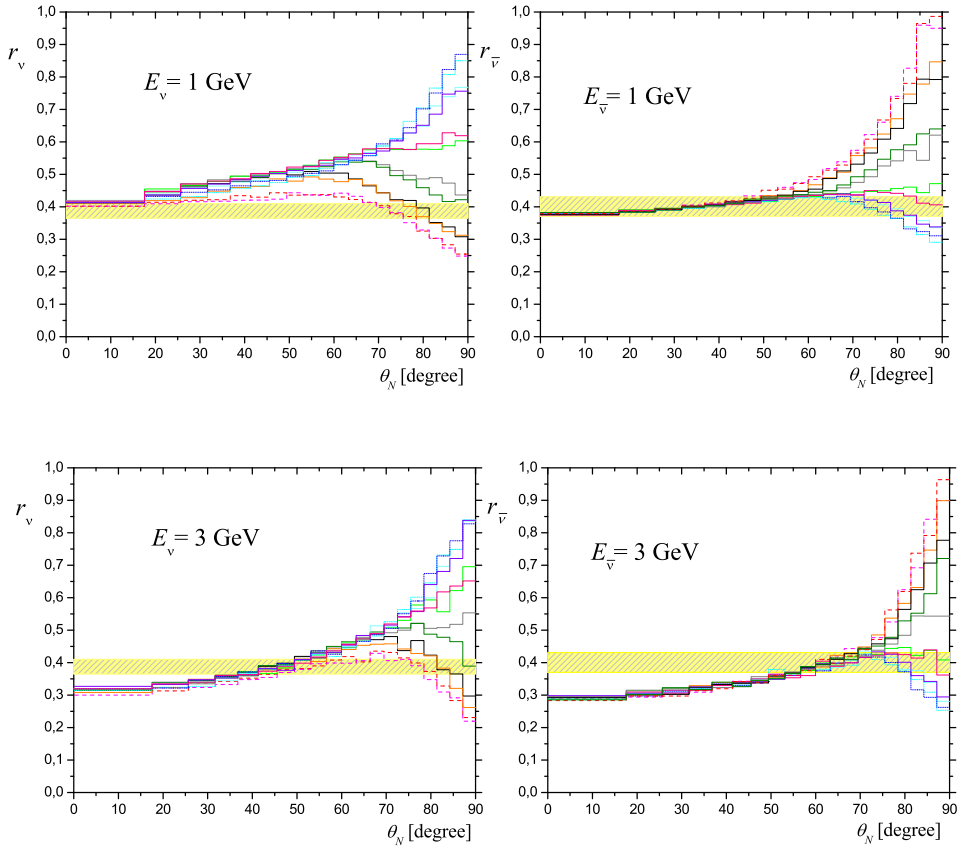

Fig. 3. Dependances of "low-energy" neutrinos (left) and antineutrinos (right) flux ratios at INO site on the nadir angle for 12 different azimuthal directions with 30° step are shown in comparison with $\sin^2\vartheta_{\rm atm}$ values for the NH (left) and the IH (right). The reddish (dashed) curves correspond to neutrinos coming from the East, while the bluish (dotted) curves – from the West.

neutrinos coming from the East, while the bluish (dotted) curves – from the West.

The East-West asymmetry is more pronounced for "low-energy" neutrinos at 1 and 3 GeV (Fig. 3) than for "high-energy" neutrinos at 6 and 10.6 GeV (Fig. 4) and for the neutrinos (left panels) than for the antineutrinos (right panels). The low-energy neutrinos are produced by the low-energy primary CRs, which are more affected by the geomagnetic fields. In its turn, neutrino–antineutrino difference is due to the fact that positively charged primaries produce mainly neutrinos than antineutrinos. However, the East-West asymmetry cannot be used to enhance the matter effect, since it is significant for

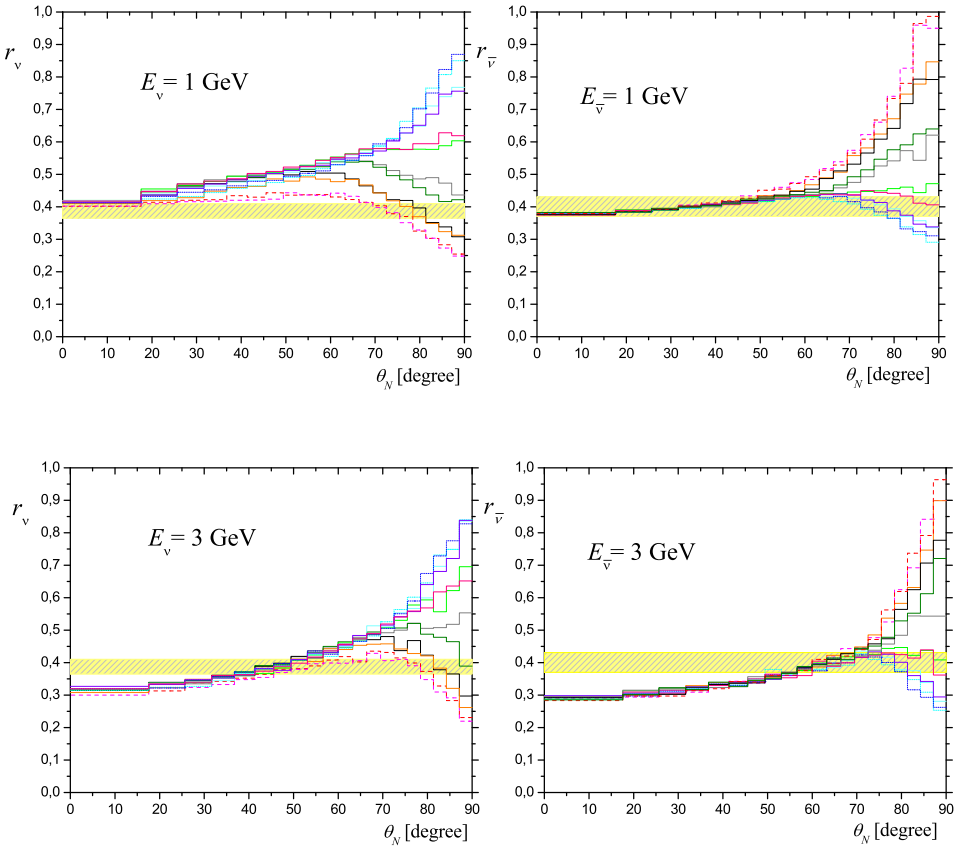

Fig. 4. Dependances of "high-energy" neutrinos (left) and antineutrinos (right) flux ratios at INO site on the nadir angle for 12 different azimuthal directions with 30° step are shown in comparison with $\sin^2\vartheta_{\rm atm}$ values for the NH (left) and the IH (right). The reddish (dashed) curves correspond to neutrinos coming from the East, while the bluish (dotted) curves – from the West.

low-energy and near horizontal arriving neutrinos. Therefore, in the following we will use averaged fluxes on the azimuthal angle.

The best-fit values of $\sin^2\vartheta_{\rm atm}$ from the global three-neutrino oscillation analysis (Fogli 2012) are shown for the NH in the neutrino case (left panels) and for the IH in the antineutrino case (right panels). It can be seen from Fig. 4 that at the resonant neutrino energy, 6 GeV, the factor $\sin^2\vartheta_{\rm atm}/r - 1$ can be close to 1 for upward going neutrinos and does not suppress the matter effect.

2.2 Flux ratios for different sites

Although the atmospheric neutrino fluxes depend strongly on the detector site, the flux ratios seem to be more place independent. In Fig. 5 and Fig. 6 flux ratios for different sites to the INO location for upward going neutrinos are compared.

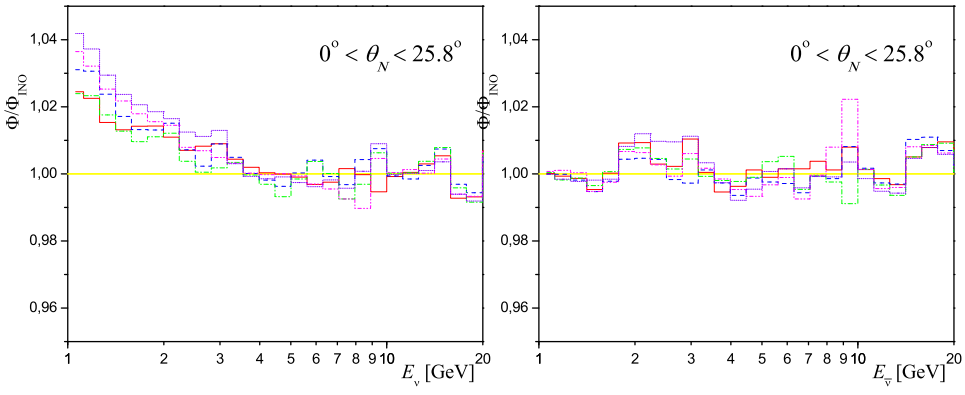

Fig. 5. The ratios of the fluxes at Kamiokande (solid), Fréjus (dashed), Gran Sasso (dash-dotted), Sudbury Neutrino Observatory (SNO) (dash-double dotted) and Soudan (dotted) to the INO location are shown as a function of the neutrino energy for the nadir angles $0.9 < \cos\theta_N < 1$.

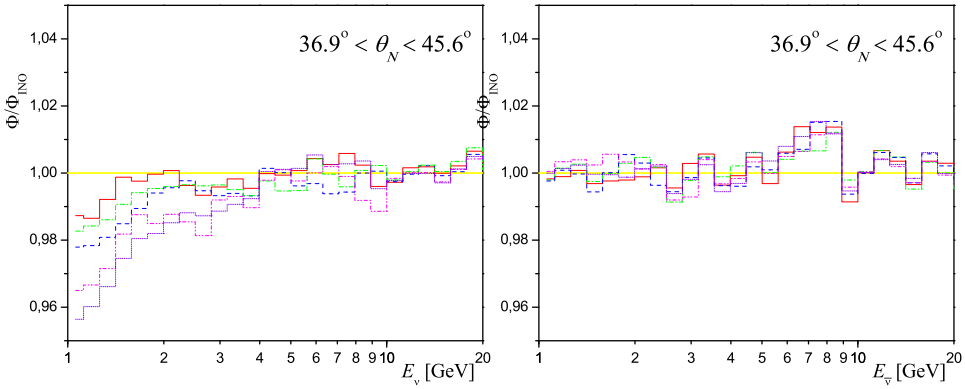

Fig. 6. Maximal deviations of the ratios for different sites (as in Fig. 5) to the INO location as a function of the neutrino energy for the nadir angles $0.7 < \cos\theta_N < 0.8$ are shown.

Only azimuthal angle bins with maximal deviations from 1 are shown in the figures. However, in the resonant energy region all calculated flux ratios

for different sites show approximately the same values within 1% accepted uncertainty (Barr 2006). On the other hand the antineutrino flux ratios show an agreement for different sites in the entire presented energy region. It means that our analysis of neutrino flux ratios can have more universal character than only for one site and with calculation by a particular group. Nevertheless, it is also obvious that our analysis results are valid only in a narrow region of parameters of interest.

2.3 Energy distributions

In order to predict neutrino flux ratios for different energies and propagation directions, we should analyse the corresponding distributions. In Fig. 7 we compare calculations of different groups for neutrino (left) and antineutrino (right) flux ratios as a function of the neutrino energy for upward going neutrinos $0.9 < \cos\theta_N < 1$.

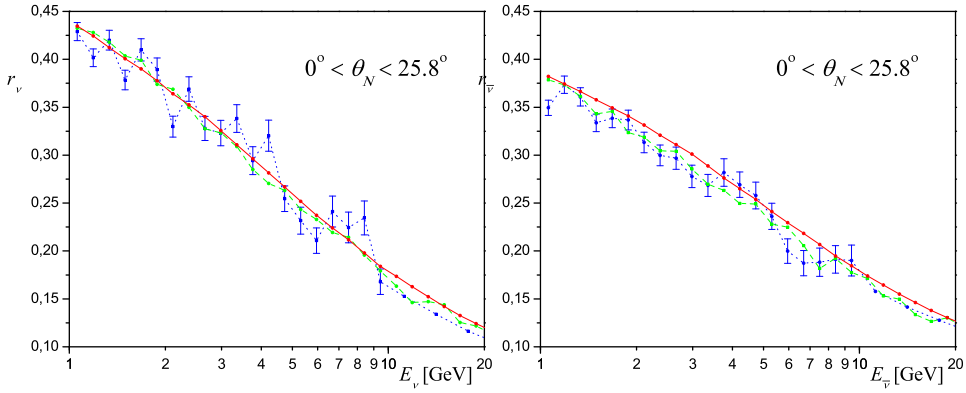

Fig. 7. The neutrino (left) and antineutrino (right) flux ratios as function of the neutrino energy for upward going neutrinos $0.9 < \cos\theta_N < 1$ calculated by Honda (2011) (solid), Barr (2004) (dotted interpolation curves with corresponding error bars) and Battistoni (2003) (dashed).

It can be seen from the figures that the most smooth distributions are provided by Honda (2011) calculations. Although Bartol group (Barr 2004) calculations are in agreement with other calculations within presented uncertainties, their distributions are extremely non-monotonic. The FLUKA Monte Carlo model gives more close agreement with Honda (2011) calculations, but still possesses significant statistical deviations.

Taken into account all these facts we will use in the following only the most precise statistically Honda (2011) calculation for INO site averaged over azimuthal angles and solar cycle. The Honda (2011) tables include also calculations with and without mountains over the detector. As far as we are interested only for upward going neutrinos both tables in this part should give the same numbers within their statistical uncertainties.

2.4 Flux fits

In this subsection we present useful parametrization of the neutrino flux ratios for the interested energy region (1 GeV $< E_\nu <$ 20 GeV) and the nadir angles ($0^\circ < \theta_N < 72.5^\circ$). We have used Honda (2011) tables for INO site, which contain fine detalization in neutrino energy (20 bins per decade in log-scale) and nadir (or zenith) angle (40 equidistant bins in $\cos\theta_N$).

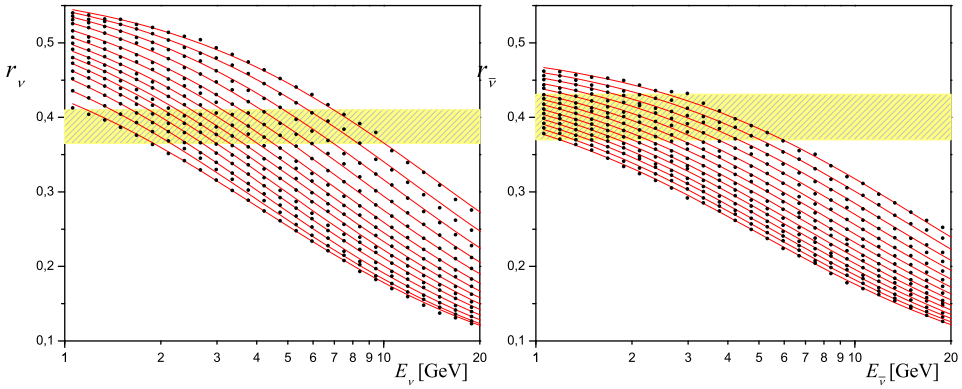

Fig. 8. The data sets of flux ratios in nadir angles and their fits over neutrino (left) and antineutrino (right) energy are shown in comparison with $\sin^2\vartheta_{\rm atm}$ values for the NH in the neutrino case and for the IH in the antineutrino case. The flux ratio magnitude is increasing with nadir angle for the same neutrino energy.

In Fig. 8 we presented 14 data sets of flux ratios in nadir angles from 0° up to 72.5° (with 0.05 step in $\cos\theta_N$) for neutrinos (left) and antineutrinos (right) as functions of the neutrino energy. We have observed that monotonically decreasing with energy neutrino flux ratios at fixed nadir angle can be fitted by the two-parametric function:

$$r(E_\nu, \cos\theta_N) = 0.04 + \frac{\mathrm{par1}(\cos\theta_N)}{E_\nu + \mathrm{par2}(\cos\theta_N)}. \tag{24}$$

In its turn the parameters for different nadir angles can be fitted by the 4-order polynomial functions in $\cos\theta_N$:

$$\mathrm{par}\, i = c_0^i + c_1^i \cos\theta_N + c_2^i \cos^2\theta_N + c_3^i \cos^3\theta_N + c_4^i \cos^4\theta_N.$$

The corresponding coefficients for neutrino case are

$$c_0^1 = 34.9329,\ c_1^1 = 150.295,\ c_2^1 = 279.512,\ c_3^1 = 241.486,\ c_4^1 = 79.3033,$$
$$c_0^2 = 70.1079,\ c_1^2 = 316.836,\ c_2^2 = 614.109,\ c_3^2 = 549.953,\ c_3^2 = 186.836;$$

and for antineutrino case:

$$c_0^1 = 19.7784,\ c_1^1 = 63.3307,\ c_2^1 = 95.522,\ c_3^1 = 70.4154,\ c_4^1 = 20.4403,$$
$$c_0^2 = 42.1156,\ c_1^2 = 132.837,\ c_2^2 = 201.597,\ c_3^2 = 150.395,\ c_4^2 = 44.4331.$$

Conclusion

In this paper we have analysed the properties of neutrino fluxes which have originated from cosmic rays interactions in the Earth's atmosphere. Upward going neutrinos propagating through the Earth can undergo oscillation phenomena in matter at some energy values depending on neutrino parameters and the Earth's profile. Therefore, knowledge of neutrino fluxes in specific directions and energy region can help in determination of the unknown yet neutrino parameters.

The crucial value in determination of neutrino parameters through the matter effect is the electron to muon neutrino flux ratio. We have obtained useful analytical formulae for it.

References

Abe K. et al. (Super-Kamiokande Collaboration), 2011, *Phys. Rev. Lett.* 107, 241801
Abe K. et al. (Super-Kamiokande Collaboration), 2006, *Phys. Rev. Lett.* 97, 171801 Phys.Rev.Lett. 107 (2011) 181802, arXiv:1108.0015 [hep-ex].
Adriani O. et al. (PAMELA Collaboration), 2009, *Phys. Rev. Lett.* 102, 051101
Alcaraz J. et al. (AMS Collaboration), 2000, *Phys. Lett.* B494, 193–202
Allison W. W. M. et al. (Soudan Collaboration), 1997, *Phys. Lett.* B391, 491
Ambrosio M. et al. (MACRO Collaboration), 1998, *Phys. Lett.* B434, 451
An F. P. et al. (Daya Bay Collaboration), 2012, *Phys. Rev. Lett.* 108, 171803
Athar M. S. et al., 2013, *Phys. Lett.* B718, 1375
Aubert J. J. et al. (E598 Collaboration), 1974, *Phys. Rev. Lett.* 33, 1404
Augustin J. E. et al. (SLAC-SP-017 Collaboration), 1974, *Phys. Rev. Lett.* 33, 1406
Barbieri R., Dolgov A., 1991, *Nucl. Phys.* B349, 743-753
Barr G. D. et al., 2004, *Phys. Rev.* D70, 023006; `http://www-pnp.physics.ox.ac.uk/~barr/fluxfiles/`
Barr G. D. et al., 2006, *Phys. Rev.* D74, 094009
Battistoni G. et al., 2003, *Astropart. Phys.* 19, 269-290; `http://pcbat1.mi.infn.it/~battist/neutrino.html`.
Becker-Szendy R. et al. (IMB Collaboration), 1992, *Phys. Rev.* D46, 3720
Berezhko E. G., Völk H. J., 2007, arXiv:0704.1715 [astro-ph]
Blasi P., Amato E., 2012, *JCAP* 01, 010
Boezio M. et al. (CAPRICE Collaboration), 2003, *Phys. Rev.* D67, 072003
Casper D. et al. (IMB Collaboration), 1991, *Phys. Rev. Lett.* 66, 2561
Catanesi M. G. et al. (HARP Collaboration), 2008, Astropart. Phys. 30, 124-132
Chizhov M. V., Petcov S. T., 1999, *Phys. Rev. Lett.* 83, 1096-1099
Chizhov M., 2001, *Nuclear Physics* B (Proc. Suppl.) 100, 133-135
Davis R. et al., 1972, Proc. Conf. Neutrino 72, Hungary, vol.I p. 29
Finlay C. C. et al., 2010, Geophys. J. Int. 183, 1216-1230; `http://www.ngdc.noaa.gov/IAGA/vmod/igrf.html`
Fogli G. L. et al., 2012, *Phys. Rev.* D86, 013012, arXiv:1205.5254.
Fukuda Y. et al. (Kamiokande Collaboration), 1994, *Phys. Lett.* B335, 237
Fukuda Y. et al. (Super-Kamiokande Collaboration), 1998, *Phys. Rev. Lett.* 81, 1562-1567
Fukuda S. et al. (Super-Kamiokande Collaboration), 2000, *Phys. Rev. Lett.* 85, 3999
Gaisser T. K., 2005, *Phys. Scripta* T121, 51-56
Hänssgen K., Ranft J., 1986, *Comput. Phys.* 39, 53-70
Hirata K. S. et al. (Kamiokande Collaboration), 1988, *Phys. Lett.* B205, 416
Hirata K. S. et al. (Kamiokande Collaboration), 1992, *Phys. Lett.* B280, 146
Honda M. et al., 1995, *Phys. Rev.* D52, 4985-5005
Honda M. et al., 2007, *Phys. Rev.* D75, 043006
Honda M. et al., 2011, *Phys. Rev.* D83, 123001; `http://icrr.u-tokyo.ac.jp/~mhonda`
Kang H., 2011, arXiv:1102.3123 [astro-ph.HE]
Kasahara K., Torii S., 1991, —em Comput. Phys. Commun. 64, 109-120
Maki Z., Nakagawa M. and Sakata S., 1962, *Prog. Theor. Phys.* 28, 870
Mikheyev S. P., Smirnov A. Yu., 1985, *Sov. J. Nucl. Phys.* 42, 913
Niita K. et al., 2006, *Radiation Measurements* 41, 1080
Nilsson-Almqvist B., Stenlund E., 1987, *Comput. Commun.* 43, 387
Niu K., Proc. Japan Acad. B 84 (2008) 1.
Page D. E., Marsden R. G. eds., 1997, *The Heliosphere at Solar Minimum* (Pergamon Press)
Picone J. M. et al., 2002, *J. Geophys. Res.* 107, 1468
Pontecorvo B., 1957, *Zh. Eksp. Teor. Fiz.* 33, 549
Pontecorvo B., 1958, *Zh. Eksp. Teor. Fiz.* 34, 247
Roesler S., Engel R., Ranft J., 2000, hep-ph/0012252; `http://sroesler.web.cern.ch/sroesler/dpmjet3.html`.
Sanuki T. et al. (BESS Collaboration), 2000, *Astrophys. J.* 545, 1135
Wolfenstein L., 1978, *Phys. Rev.* D17,2369